Controllability of nonlinear epileptic-seizure spreading dynamics in large-scale subject-specific brain networks

Supplementary Material

S. Amin Moosavi, Jordan S. Feldman, Wilson Truccolo
Brown University, Providence, RI, USA

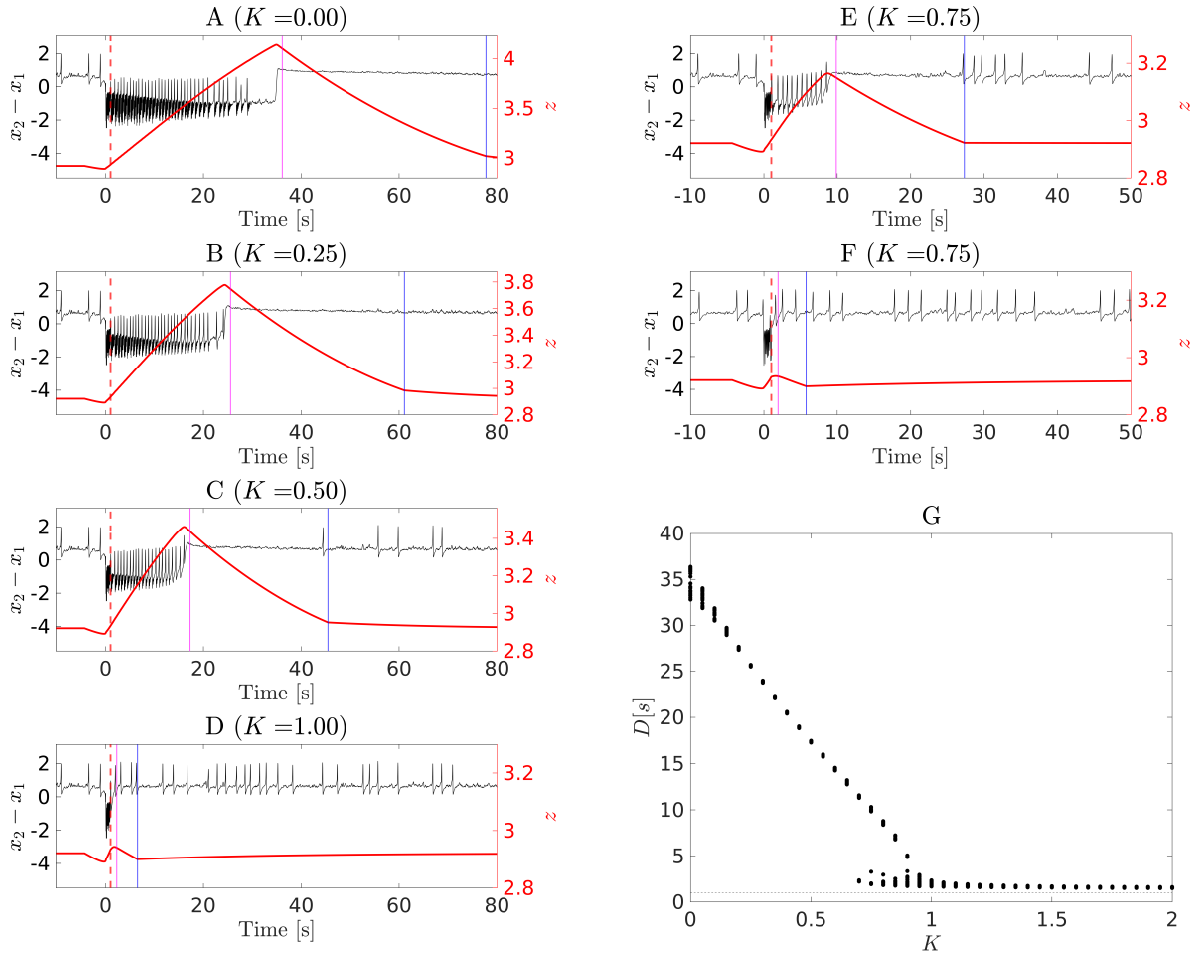

Supp Fig 1: **Linear feedback control of stochastic single-node Epileptor with actuation only on the x_1 variable.** Same conventions and simulation setup as in Figure 4. **A** Seizure dynamics without feedback control ($K = 0$). **B-D** By increasing the control gain K, the duration of the seizure decreases but the amplitude of the ictal spikes, generated by the ictal oscillations in the (x_2, y_2) subsystem, remains large during the seizure. The interictal spikes reappear after the intrinsic refractory period, i.e. when the z variable gets close to its preictal value. **E,F** As shown before, the duration of a seizure can differ substantially for different stochastic realizations of the same Epileptor model and control gain. **G** Duration of seizure D plotted versus the control gain K. Each dot relates to a stochastic realization. 30 stochastic realizations were simulated for each K value. As seizure duration decreases with increasing K, there is also bimodality for $0.7 < K < 0.9$. Seizure duration starts to saturate close to the control onset latency of 1 second (gray dashed line) after $K > 0.9$. Overall, compared with Figure 4, actuation only on x_1 has similar effects on seizure duration as actuation on both x_1 and x_2 variables, but the ictal spikes remain large during the seizure.

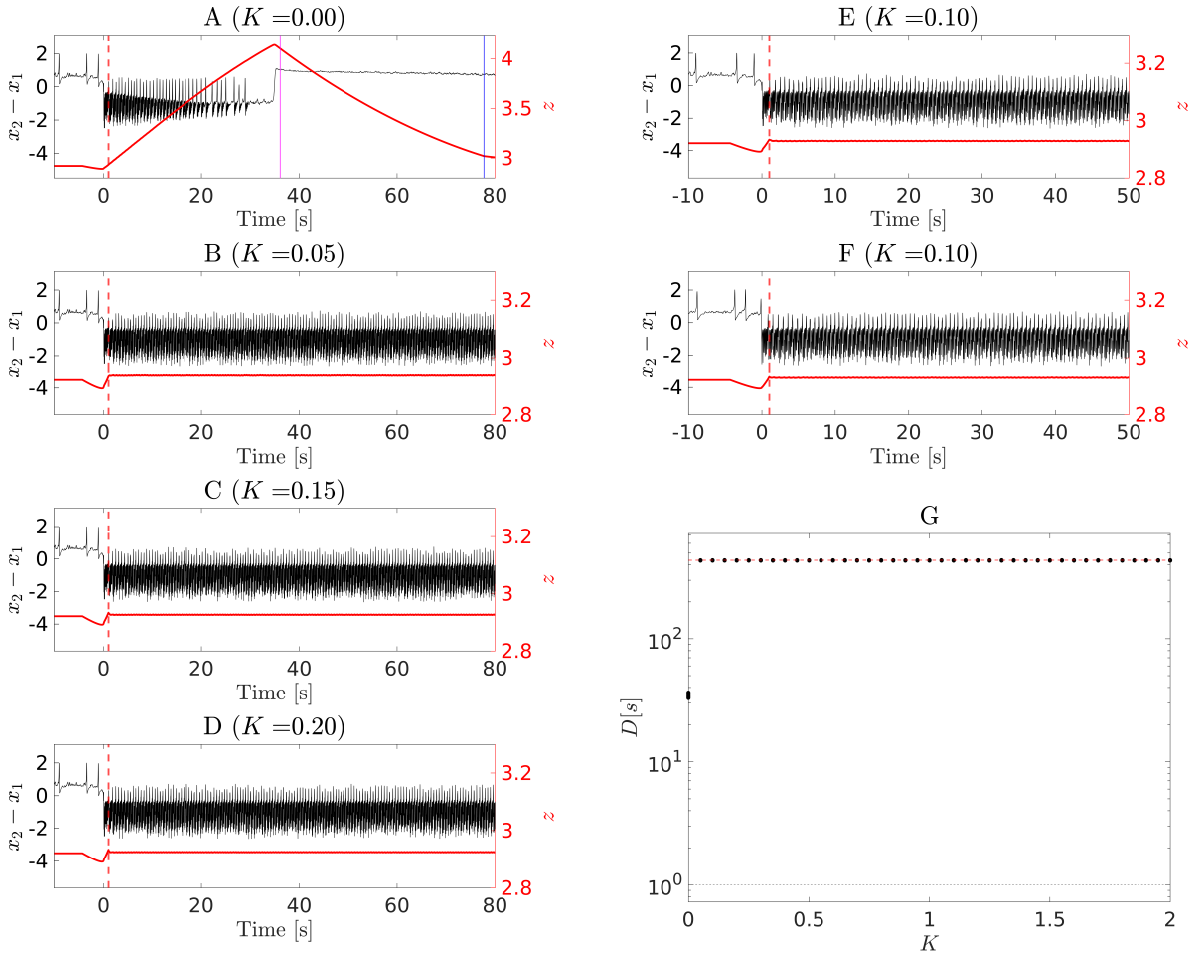

Supp Fig 2: **Linear feedback control of stochastic single-node Epileptor with actuation only on the z variable.** Same conventions and simulation setup as in Figure 4. **A** Seizure dynamics without feedback control ($K = 0$). **B-F** Actuation on the z variable with a control target set to a preictal z value not only fails to reduce seizure duration but even prevent the seizure from self-terminating. By stabilizing z near the preictal z^* value, feedback control also maintains the ictal limit cycle indefinitely. In this stabilized seizure state, x_1 oscillates around a mean value $\bar{x}_1$ and z settles (Eq. **??**) to $z_s = \frac{4(\bar{x}_1 - x_0) + \tau_0 K z^*}{1 + \tau_0 K}$. Because $\tau_0 \gg 1$, $z_s \approx z^*$ as expected. **G** The duration of seizures D is maxed at the simulation time for $K > 0$. In summary, because of the hysteresis effects on the Epileptor dynamics as z evolves, a more complex design of control targets in terms of other target steady-states or target paths would be required for successful seizure termination.

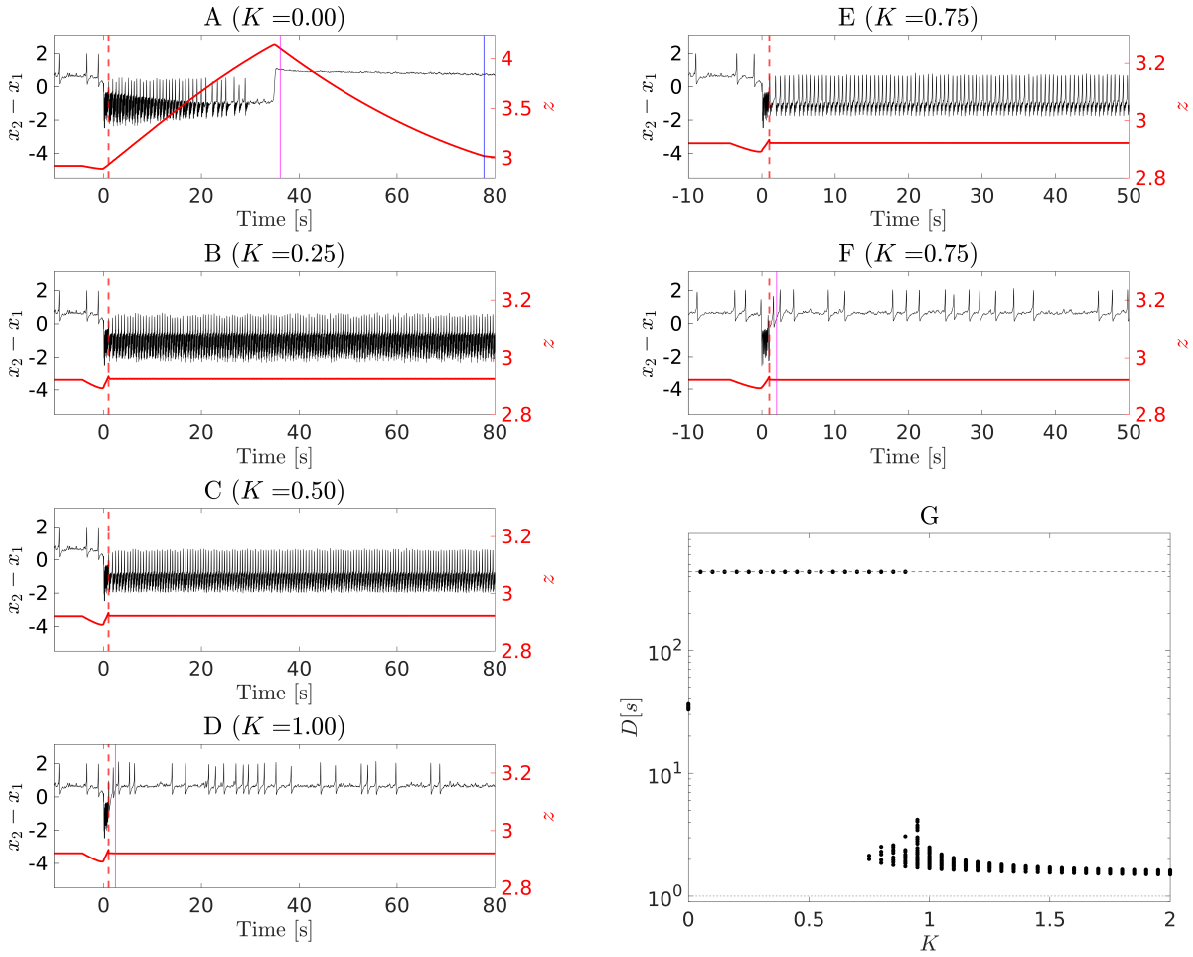

Supp Fig 3: **Linear feedback control of stochastic single-node Epileptor with actuation on both the x_1 and z variables.** Same conventions and simulation setup as in Figure 4. **A** Seizure dynamics without feedback control ($K = 0$). **B,C** For small control gains (e.g. $K = 0.25, 0.5$), this actuation approach fails, preventing even the self-termination of the seizure, as seen before (Supp. Fig. 2). Actuation on x_1 is not strong enough to push the x_1 and y_1 dynamics away from the stable ictal limit cycle. **D** For larger control gains (e.g. $K >= 1$), feedback control successfully terminates the seizure. **E,F** For intermediate K values, successful control of seizure termination depends on the stochastic realization as seen before (Supp. Fig. 1). **G** Seizure duration D is maxed at the simulation time for $K < 0.7$ and bimodality is observed for $0.7 < K < 1$. For comparasion purposes with (B,C,E), feedback control is kept on over the entire simulation time in (D,F).

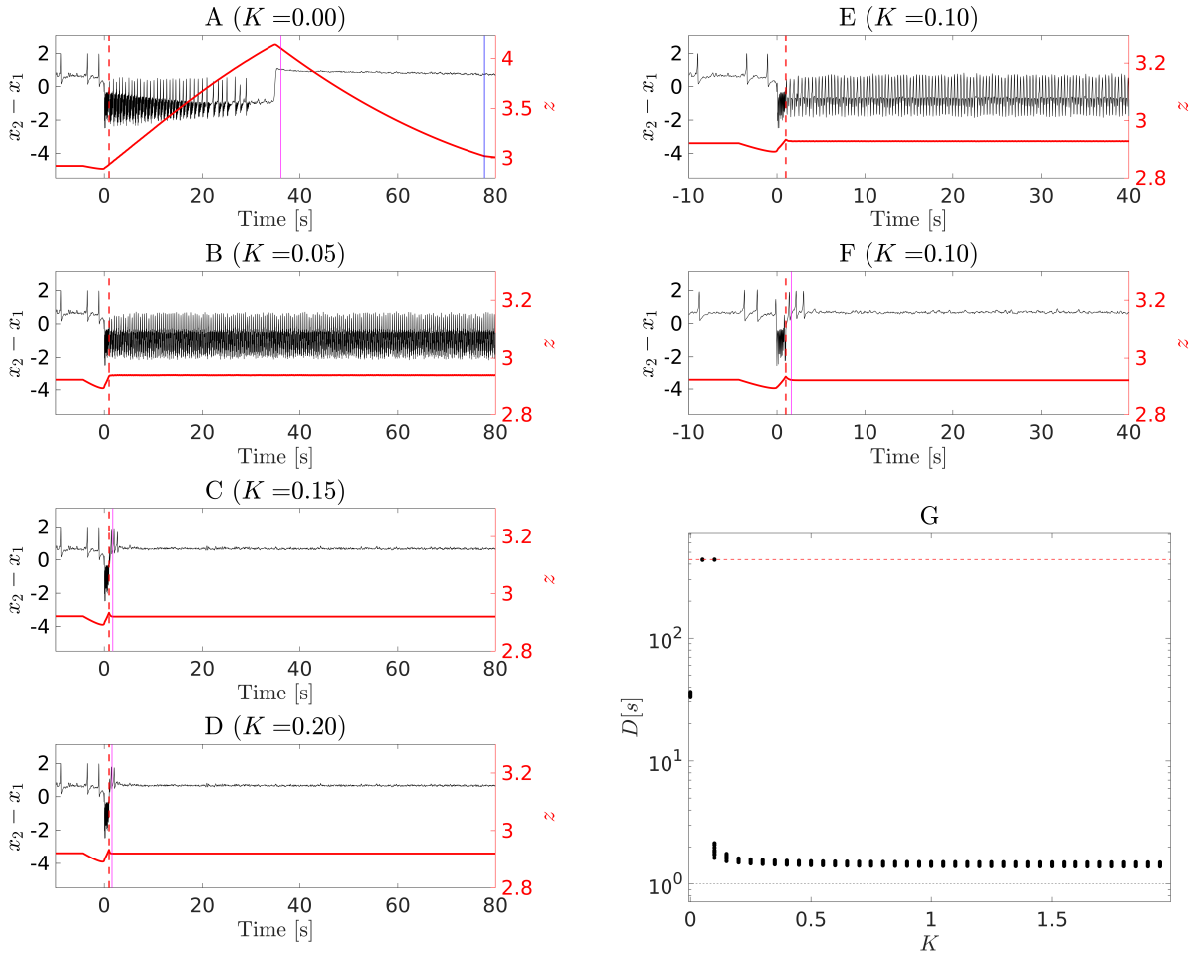

Supp Fig 4: **Linear feedback control of stochastic single-node Epileptor with actuation on all the variables.** Same conventions and simulation setup as in Figure 4. **A** Seizure dynamics without feedback control ($K = 0$). **B** For small enough control gains (e.g. $K = 0.05$), feedback control fails, preventing even seizure self-termination. **C,D** For higher control gains (e.g. $K = 0.15, 0.20$), feedback control can successfully terminate the seizure. **E,F** For control gains near $K = 0.1$, feedback control success depends on the stochastic realization. **G** Seizure duration D is maxed at the simulation time for small $K < 0.1$. For larger control gain values (e.g. $K > 0.10$), feedback control succeeds by terminating the seizure soon after control onset. For comparasion purposes with (B), feedback control is kept on over the entire simulation time in (C-F).

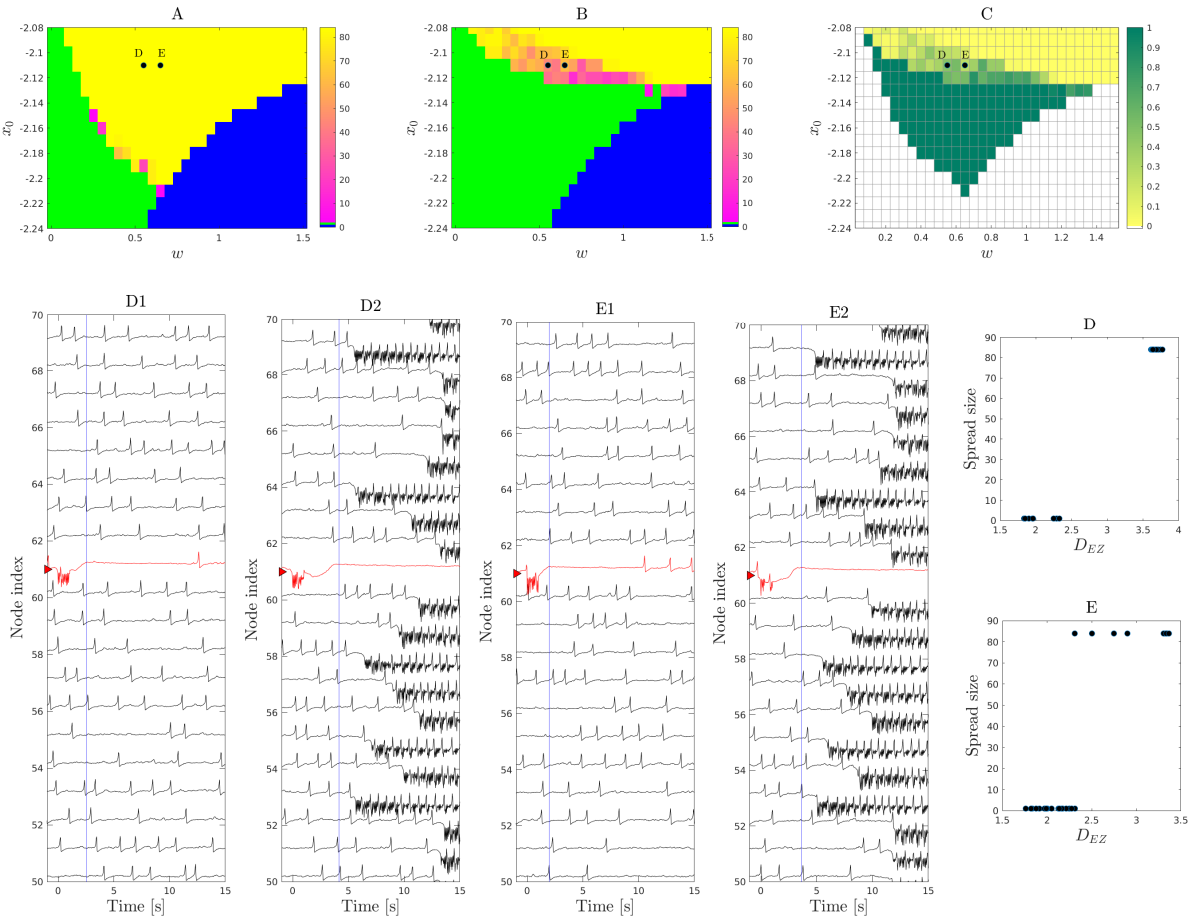

Supp Fig 5: **Spread size bimodality in stochastic subject-specific Epileptor networks: bimodality in spread size distributions arises from the bimodality in seizure duration in the (seizure onset) EZ node. A** Phase diagram of seizure spread size for the subject-specific (P1) Epileptor network. Same conventions as in previous figures. **B** Phase diagram of seizure spread size for the same Epileptor network as in (A) but now under linear feedback control, with gain $K = 0.75$ and actuation only at the EZ node. Near the phase transition boundary there is a region of average partial spread (across 30 stochastic realizations). **C** The corresponding controllability diagram for (B). **D1, D2** Two examples of the Epileptor network activity ($x_2 - x_1$) where spread control succeeds (D1) and fails (D2), both corresponding to the same point D in the (w, x_0) parameter space as shown in (A-C). Activity of the EZ node is indicated by the red color. The blue vertical line indicates the time of seizure termination and feedback control offsetin the EZ node. The seizure duration is clearly longer in the case when full spread occurs (D2). **E1,E2** Two additional examples for the point E in the (w, x_0) parameter space. Same conventios as in (D1,D2). **D,E** Spread size, even under feedback control, is strongly dependent on the duration of the seizure (D_{EZ}) in the (seizure onset) EZ node, with a very sharp transition between no spread and full spread as shown in the two plots correspoding to the point D and E in the (w, x_0) parameter space.

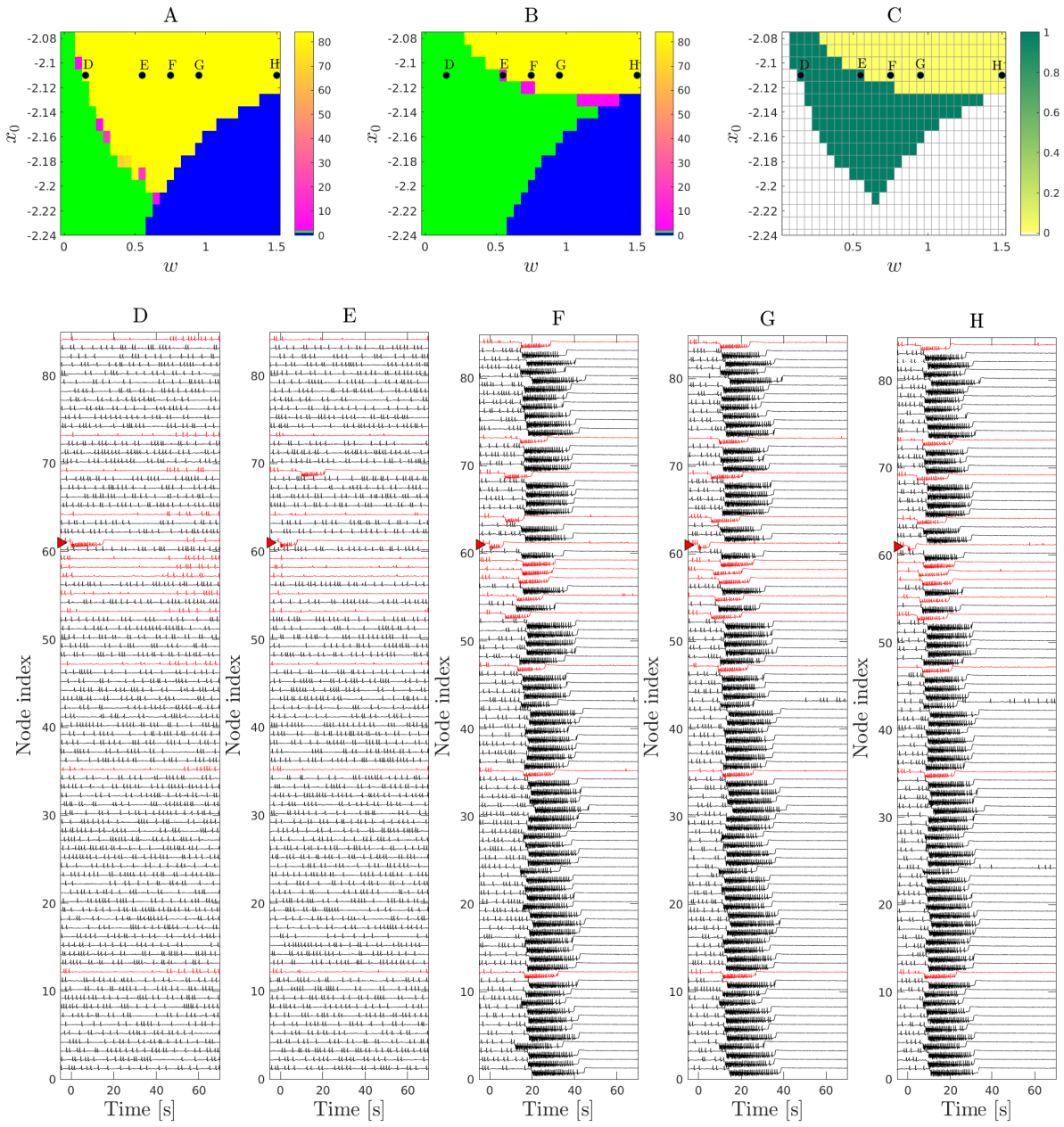

Supp Fig 6: **Linear feedback control of subject-specific Epileptor networks with simultaneous actuation at the (seizure onset) EZ node and an optimal subset of non-EZ nodes.** Same conventions as in Figure 5. The optimal subset consisted of 12 non-EZ nodes selected according to corresponding ranked components of the leading eigenvector of the Jacobian matrix (Methods). Control gain was set to $K = 0.25$ and control onset latency to 1 second after seizure onset in the EZ node. **A** Phase diagram of the subject-specific (P1) Epileptor network without feedback control. **B** Same as in (A) but under linear feedback control. **C** The corresponding controllability diagram reflecting the partial controllability in the (w, x_0) parameter space. **D, E, F, G, H** Examples of Epileptor network activity $(x_2 - x_1)$ related to the corresponding points D, E, F, G, H in the (w, x_0) space as indicated in (A-C). Activity in all of the actuated nodes is displayed in red, with the (seizure onset) EZ node indicated by the red triangle.

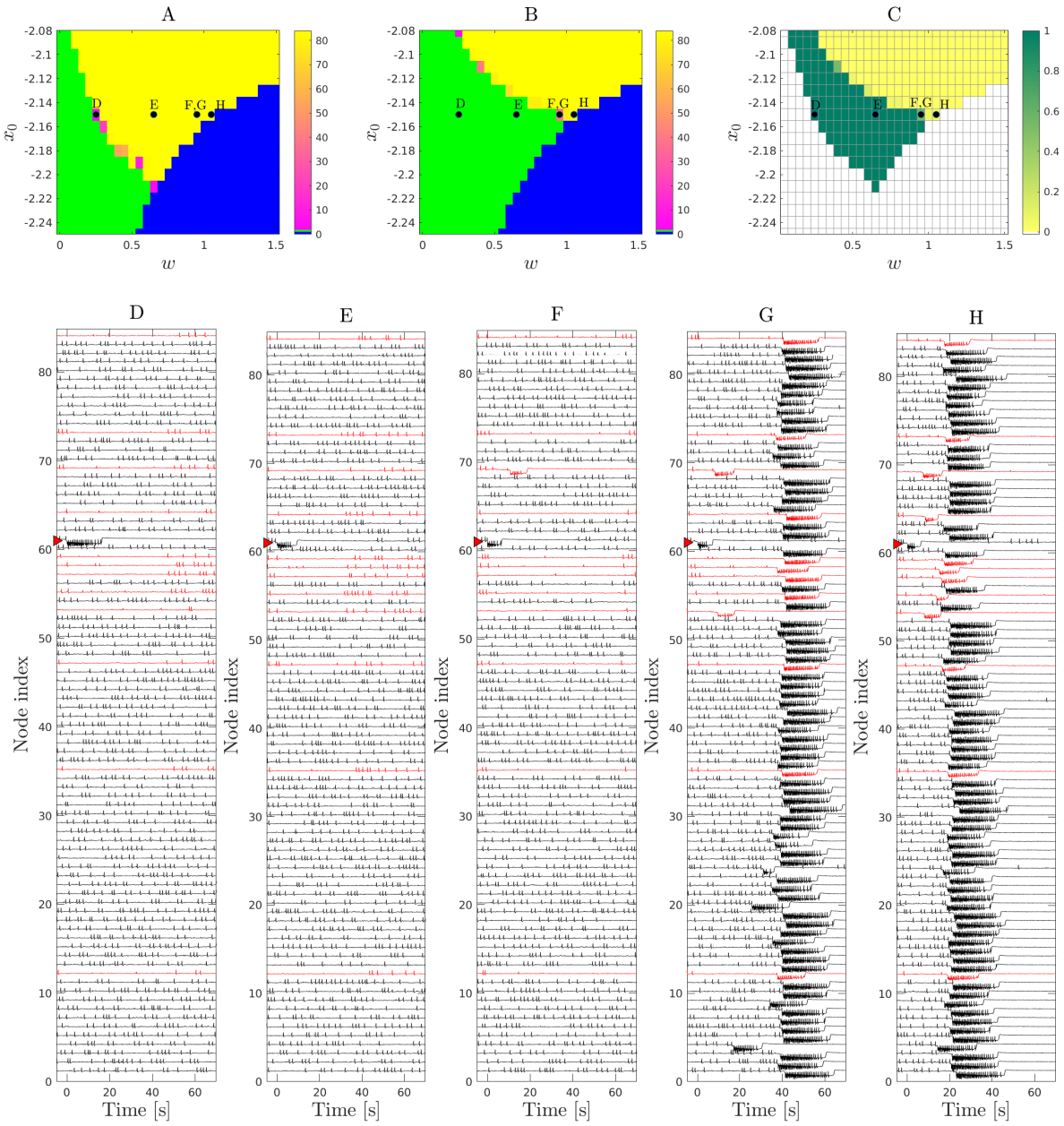

Supp Fig 7: **Linear feedback control of subject-specific Epileptor networks with actuation only at an optimal subset of non-EZ nodes.** Same conventions as in Figure 5. **A** Phase diagram of the subject-specific (P1) Epileptor network without feedback control. **B** Same as in (A) but with linear feedback control and actuation at only an optimal subset of 12 non-EZ nodes selected according to corresponding ranked components of the leading eigenvector of the Jacobian matrix (Methods). Control gain was set to $K = 0.25$ and control onset latency to 1 second after seizure onset in the EZ node. **C** The corresponding controllability diagram indicating partial controllability. **D, E, F, G, H** Examples of Epileptor network activity $(x_2 - x_1)$ related to the corresponding points D, E, F, G, H in the (w, x_0) space as indicated in (A-C). Activity in all of the actuated nodes is displayed in red, with the (seizure onset) EZ node indicated by the red triangle.

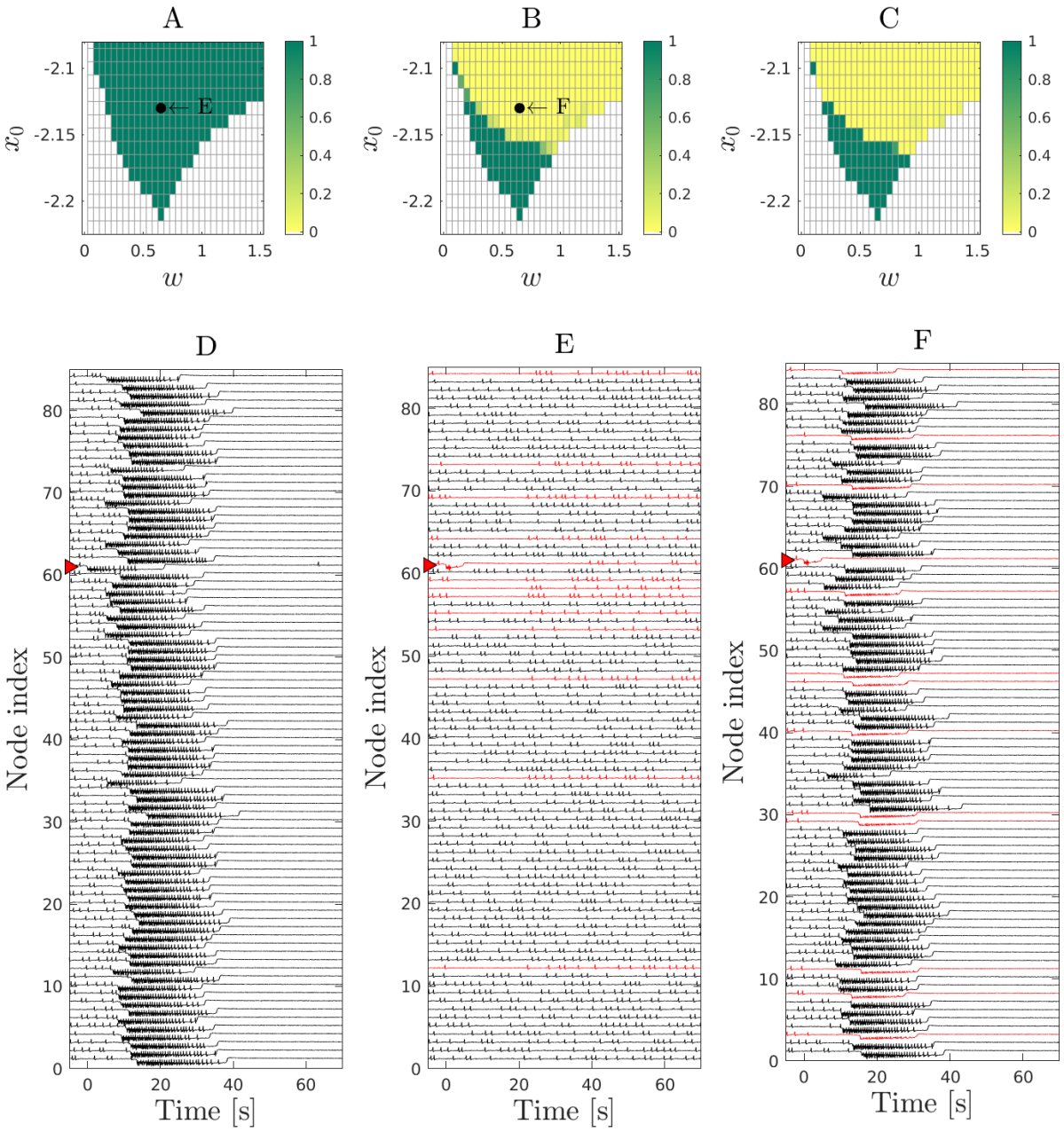

Supp Fig 8: **Linear feedback control of subject-specific Epileptor networks with simultaneous actuation at the (seizure onset) EZ node and a subset of non-EZ nodes: comparing optimal versus random subset selection. A** Controllability diagram with simultaneous actuation at the (seizure onset) EZ node and an optimal subset of 12 non-EZ nodes in the (P1) network. Control gain was set to $K = 0.5$ and control onset latency to 1 second after seizure onset in the EZ node. The diagram shows perfect controllability in all of the (w, x_0) parameter space. Optimal subset selection was based the ranked components of the leading eigenvector of the Jacobian matrix (Methods). **B** Same as in (A), except that the optimal subset is replaced by 12 randomly selected non-EZ nodes. Specifically, for each of the 30 stochastic realizations, 12 non-EZ nodes were randomly selected for actuation. (Continuation on next page ...)

(Supp. Fig. 8 continuation) In contrast to (A), now the region of successful spread preventions has been greatly reduced. **C** Same as in (A), except that actuation was restricted to only the EZ node, under the same network, initial conditions and stochastic noise realizations. Clearly, in comparison to (B), actuation at a randomly selected subset did not significantly contribute to controllability. **D** An example of full seizure spread in the same Epileptor network without linear feedback control for the point E in the (w, x_0) parameter space as indicated in (A). Node activity corresponds to the observable $(x_2 - x_1)$. **E** Same as in (D) but with linear feedback control actuation at both the ictal EZ node and the optimal subset of 12 non-EZ nodes. **F** Same as in (E), except that the 12 non-EZ nodes were randomly selected. For clarity, the corresponding (w, x_0) point is indicated by both E and F in (A,B), respectively. The time series of the actuated nodes are shown in red color and the EZ node is indicated by the triangle. We note that the probability of selecting the 12 top nodes ranked according to the Jacobian leading eigenvector in a network with one EZ and $N-1$ non-EZ nodes is $\frac{(N-13)!12!}{(N-1)!}$; that is approximately 1.0325×10^{-14} for $N = 84$. (See additional details in the main text.)

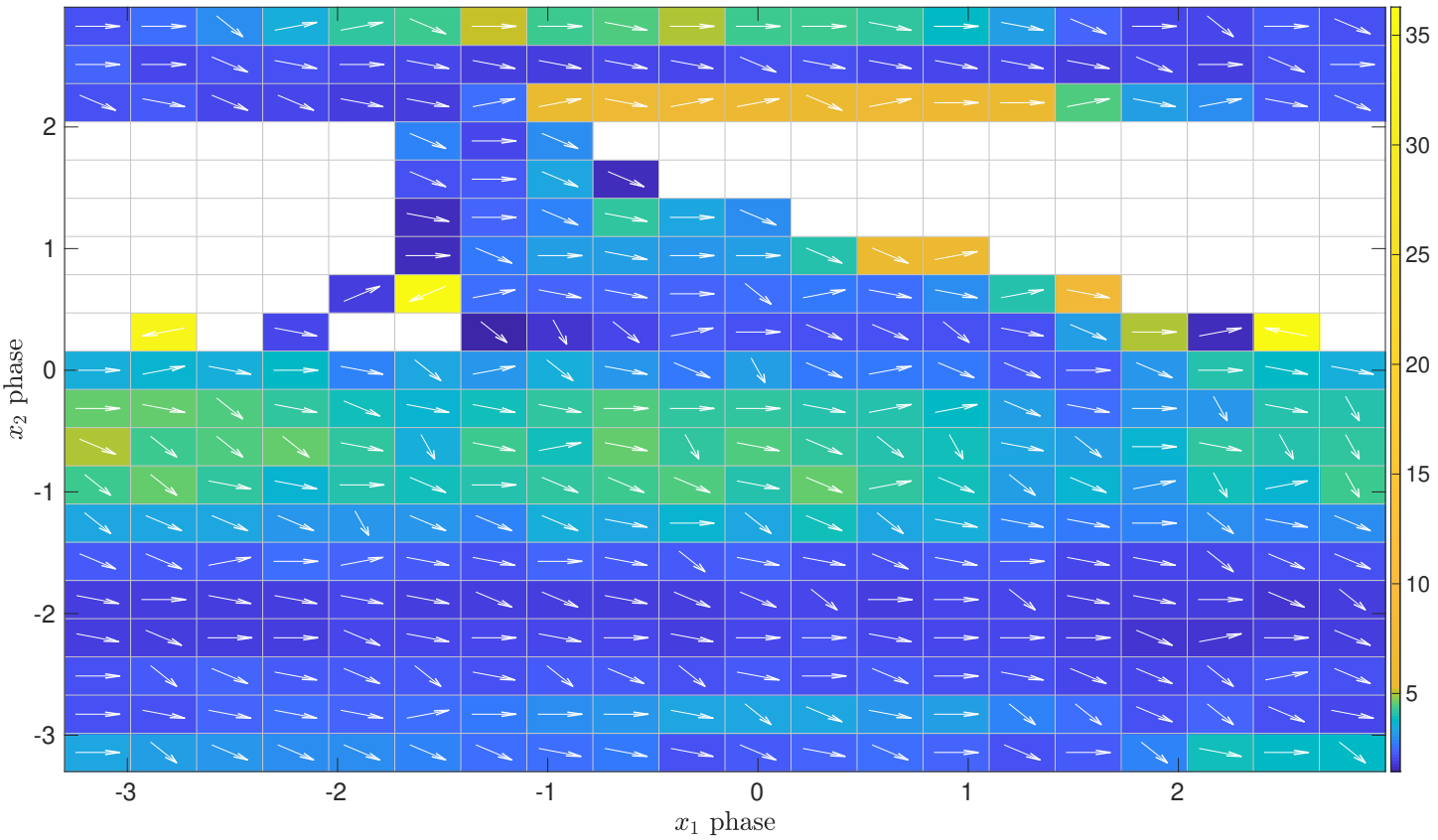

Supp Fig 9: **Nonlinear pulse perturbations with varying pulse onset time with respect to ongoing ictal oscillations and varying pulse direction.** We ran stochastic simulations of single-node Epileptor seizure dynamics. Pulses were delivered at each binned phase of the x_1 oscillation and the x_2 oscillation. Bins ranged from $-\pi$ to π and had width $\pi/10$. Minimum pulse onset latency was set to 1 second after seizure onset and considered only the first 10 seconds of the seizure in this analysis. (See main text for additional details.) In addition, different variations for the magnitude and direction of the pulse vector were examined. Amplitudes 4, 8, 12, 16 were examined with this figure for amplitude 16. The pulse vector angle was binned from 0 to 2π with phase bins of width $\pi/10$. (The choices in magnitude and direction determined by the amplitudes for the x_1 and x_2 component of the pulse.) Thirty stochastic realizations were sampled for each condition. Blanck spaces in the grid indicate (x_1, x_2) phase bins not reached in the first 10 seconds of the seizure, as coupled oscillator dynamics prevent certain oscillator phase combinations. White arrows correspond to the direction for each phase pair that achieved the shortest average seizure duration. The colorbar indicates seizure duration in seconds. Pulses with positive and slightly negative amplitudes in the x_1 and x_2 components, respectively, were most successful in terminating the seizures. In addition, their effect was stronger when x_2 was not spiking, i.e. with phase around -2 rad. (See main text, Methods, for additional details.)

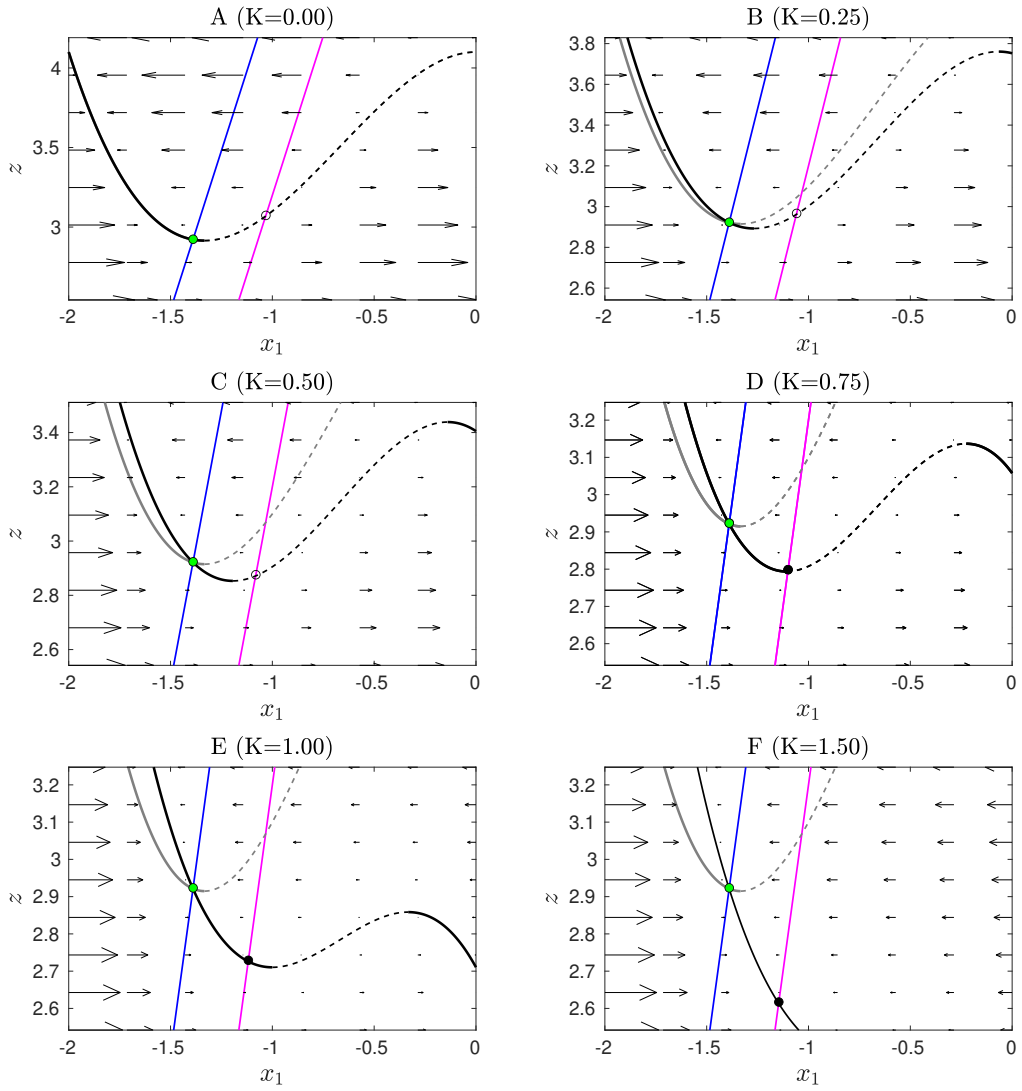

Supp Fig 10: **Linear feedback control of the deterministic single-node Epileptor ($x_1 < 0$ domain): how variations in control gain affect the number and stability of fixed points, and related vector fields. A-F** The z-nullcline based on the full 5-dimensional system (x_1, y_1, z, x_2, y_2) for the supercritical ($x_0 = -1.8 > x_{0,c}$) and subcritical ($x_0 = -2.12 < x_{0,c}$) excitability levels are indicated by the magenta and blue colors, respectively. The x_1-nullclines are indicated by the black and gray curves. The latter corresponds to the Epileptor without feedback control. Stable (unstable) branches in the x_1 correspond to regions where stable (unstable) FPs are possible in the 4-dimensional system (x_1, y_1, x_2, y_2) as the nullcline of the slowest variable z, taken as a control parameter, is translated. Solid (hollow) circles indicate stable (unstable) FPs of the full 5-dimensional model. The arrows indicate the gradient field of the x_1 variable. Due to the difference in scales, the gradient field of the z variable is not shown. It is upwards below the z-nullcline and downwards above it, indicating stability in the z direction.